

1 **Running Title:**

2 "ER-Ca²⁺ sensor STIM regulates neuropeptides required for development under nutrient
3 restriction in *Drosophila*"

4 Megha*(1), Christian Wegener (2) and Gaiti Hasan(1)

5 1. National Centre For Biological Sciences, Tata Institute for Fundamental Research,
6 Bellary Road, Bangalore 560065

7 2. Department of Neurobiology and Genetics, Theodor-Boveri-Institute, Biocenter,
8 University of Würzburg, Am Hubland, 97074 Würzburg

9 *Corresponding author; Contact: meghaphd@ncbs.res.in

10

11 ORCID:

12 Megha: 0000-0002-2968-8211

13 Christian Wegener: 0000-0003-4481-3567

14 Gaiti Hasan: 0000-0001-7194-383X

15

16 **Abstract**

17 Neuroendocrine cells communicate via neuropeptides to regulate behaviour and
18 physiology. This study examines how STIM (Stromal Interacting Molecule), an ER-Ca²⁺
19 sensor required for Store-operated Ca²⁺ entry, regulates neuropeptides required for
20 *Drosophila* development under nutrient restriction (NR). We find two STIM-regulated
21 peptides, Corazonin and short Neuropeptide F, to be required for NR larvae to complete
22 development. Further, a set of secretory DLP (Dorso lateral peptidergic) neurons which co-
23 express both peptides was identified. Partial loss of *dSTIM* caused peptide accumulation in
24 the DLPs, and reduced systemic Corazonin signalling. Upon NR, larval development
25 correlated with increased peptide levels in the DLPs, which failed to occur when *dSTIM* was
26 reduced. Comparison of systemic and cellular phenotypes associated with reduced *dSTIM*,
27 with other cellular perturbations, along with genetic rescue experiments, suggested that
28 *dSTIM* primarily compromises neuroendocrine function by interfering with neuropeptide
29 release. Under chronic stimulation, *dSTIM* also appears to regulate neuropeptide synthesis.

30

31

32 Introduction

33 Metazoan cells commonly use ionic Ca^{2+} as a second messenger in signal
34 transduction pathways. To do so, levels of cytosolic Ca^{2+} are dynamically managed. In the
35 resting state, cytosolic Ca^{2+} concentration is kept low and maintained thus by the active
36 sequestration of Ca^{2+} into various organelles, the largest of which is the ER. Upon
37 activation, ligand-activated Ca^{2+} channels on the ER, such as the ryanodine receptor or
38 inositol 1,4,5-trisphosphate receptor (IP_3R), release ER-store Ca^{2+} into the cytosol. Loss of
39 ER- Ca^{2+} causes STromal Interacting Molecule (STIM), an ER-resident transmembrane
40 protein, to dimerize and undergo structural rearrangements. This facilitates the binding of
41 STIM to Orai, a Ca^{2+} channel on the plasma membrane, whose pore now opens to allow
42 Ca^{2+} from the extracellular milieu to flow into the cytosol. This type of capacitative Ca^{2+}
43 entry is called Store-operated Ca^{2+} entry (SOCE) [1]. Of note, key components of SOCE
44 include the IP_3R , STIM and Orai, that are ubiquitously expressed in the animal kingdom,
45 underscoring the importance of SOCE to cellular functioning. Depending on cell type and
46 context, SOCE can regulate an array of cellular processes [2].

47 Neuronal function in particular is fundamentally reliant on the elevation of cytosolic
48 Ca^{2+} . By tuning the frequency and amplitude of cytosolic Ca^{2+} signals that are generated,
49 distinct stimuli can make the same neuron produce outcomes of different strengths [3]. The
50 source of the Ca^{2+} influx itself contributes to such modulation as it can either be from
51 internal ER-stores or from the external milieu, through various activity-dependent voltage
52 gated Ca^{2+} channels (VGCCs) and receptor-activated Ca^{2+} channels or a combination of the
53 two. Although the contributions of internal ER- Ca^{2+} stores to neuronal Ca^{2+} dynamics are
54 well recognized, the study of how STIM and subsequently, SOCE-mediated by it, influences
55 neuronal functioning, is as yet a nascent field.

56 Mammals have two isoforms of STIM, STIM₁ and STIM₂, both which are widely
57 expressed in the brain. As mammalian neurons also express multiple isoforms of Orai and
58 IP₃R, it follows that STIM-mediated SOCE might occur in them. Support for this comes
59 from studies in mice, where STIM₁-mediated SOCE has been reported for cerebellar
60 granule neurons [4] and isolated Purkinje neurons [5], while STIM₂-mediated SOCE has
61 been shown in cortical [6] and hippocampal neurons [7]. STIM can also have SOCE-
62 independent roles in excitable cells, that are in contrast to its role via SOCE. In rat cortical
63 neurons [8] and vascular smooth muscle cells [9], Ca²⁺ release from ER-stores prompts the
64 translocation of STIM₁ to ER-plasma membrane junctions, and binding to the L-type VGCC,
65 Ca_v1.2. Here STIM₁ inhibits Ca_v1.2 directly and causes it to be internalized, reducing the
66 long-term excitability of these cells. In cardiomyocyte-derived HL1 cells, STIM₁ binds to a
67 T-type VGCC, Ca_v1.3, to manage Ca²⁺ oscillations during contractions [10]. These studies
68 indicate that STIM regulates cytosolic Ca²⁺ dynamics in excitable cells, including neurons
69 and that an array of other proteins determines if STIM regulation results in activation or
70 inhibition of neurons. Despite knowledge of the expression of STIM₁ and STIM₂ in the
71 hypothalamus (Human Protein Atlas), the major neuroendocrine centre in vertebrates,
72 studies on STIM in neuroendocrine cells are scarce. We therefore used *Drosophila*
73 *melanogaster* (*Drosophila*), the vinegar fly, to address this gap.

74 Neuroendocrine cells possess elaborate machinery for the production, processing
75 and secretion of neuropeptides (NPs), which perhaps form the largest group of
76 evolutionarily conserved signalling agents [11,12]. Inside the brain, NPs typically modulate
77 neuronal activity and consequently, circuits; when released systemically, they act as
78 hormones. *Drosophila* is typical in having a vast repertoire of NPs that together play a role
79 in almost every aspect of its behaviour and physiology [13,14]. Consequently, NP synthesis

80 and release are highly regulated processes. As elevation in cytosolic Ca^{2+} is required for NP
81 release, a contribution for STIM-mediated SOCE to NE function was hypothesized.

82 *Drosophila* possess a single gene for STIM, IP_3R and Orai, and all three interact to
83 regulate SOCE in *Drosophila* neurons [15,16]. In dopaminergic neurons, *dSTIM* is important
84 for flight circuit maturation [15–17], with dSTIM-mediated SOCE regulating expression of a
85 number of genes, including *Ral*, which controls neuronal vesicle exocytosis [17]. In
86 glutamatergic neurons, *dSTIM* is required for development under nutritional stress and its'
87 loss results in down-regulation of several ion channel genes which ultimately control
88 neuronal excitability [18]. Further, *dSTIM* over-expression in insulin-producing NE neurons
89 could restore Ca^{2+} homeostasis in a non-autonomous manner in other neurons of an IP_3R
90 mutant [19], indicating an important role for dSTIM in NE cell output, as well as
91 compensatory interplay between IP_3R and dSTIM. At a cellular level, partial loss of dSTIM
92 impairs SOCE in *Drosophila* neurons [15,17,20] as well as mammalian neural precursor cells
93 [21]. Additionally, reducing dSTIM in *Drosophila* dopaminergic neurons attenuates KCl-
94 evoked depolarisation and as well as vesicle release [17]. Because loss of dSTIM specifically
95 in *dim^m*⁺ NE cells results in a pupariation defect on nutrient restricted (NR) media [22], we
96 used the NR paradigm as a physiologically relevant context in which to investigate STIM's
97 role in NE cells from the cellular as well as systemic perspective.

98 **Results**

99 **SOCE is required in sNPF and Crz producing cells for development under nutritional** 100 **stress**

101 Collectively, more than 20 different NPs are known to be made by the neuroendocrine cells
102 in which reducing SOCE components resulted in poor pupariation upon NR [22]. To
103 shortlist specific NPs important for this paradigm, we undertook a curated *GAL4-UAS*

104 screen. NP-GAL₄s were used to drive the knockdown of *IP₃R* (*IP₃R^{IR}*) [23], and pupariation
105 of the resulting larvae were scored on normal vs NR media (Fig. S1A). On normal food, a
106 significant reduction of pupariation was seen only with *sNPF-GAL₄* (Fig. S1A), whose
107 expression strongly correlates with neurons producing sNPF [24]. Upon NR, the largest
108 effect was seen with *sNPF-GAL₄*, followed by small but significant pupariation defect with
109 *AstA-GAL₄* and *DSK-GAL₄* (Fig. S1A). Neurons that secrete NPs may also secrete
110 neurotransmitters, therefore, a role specifically for sNPF was tested. Reducing the level of
111 *sNPF* (*sNPF^{IR}*) or reducing an enzyme required for neuropeptide processing (*amontillado*;
112 *amon^{IR}*) [25] in *sNPF-GAL₄* expressing cells, as well as a hypomorphic sNPF mutation
113 (*sNPF^{o448}*) resulted in impairment of larval development upon NR (Fig. S1B). These data
114 indicate that sNPF is required for pupariating under NR conditions.

115 *sNPF-GAL₄* expresses in large number of neurons (>300) in the larval brain [24] (Fig.
116 S1C), and also expresses in the larval midgut and epidermis. To further refine sNPF⁺
117 neurons on which we can perform cellular investigations, we tested a *Crz-GAL₄* driver. This
118 driver expresses in fewer neurons (~22), all of which express the neuropeptide Corazonin
119 (Crz). Importantly, a small subset of these, three bilateral neurons in the brain lobe, make
120 Crz and sNPF. [24] (Fig. 1A). Reducing SOCE in Crz neurons, by reducing either IP₃R or STIM
121 (*dSTIM^{IR}*) [15,16] or over-expressing a dominant-negative version of Orai (*Orai^{F180A}*) [26],
122 resulted in reduced pupariation on NR (Fig. 1B). The absence of a developmental defect on
123 normal food suggests that SOCE in these neurons is primarily required to survive NR.

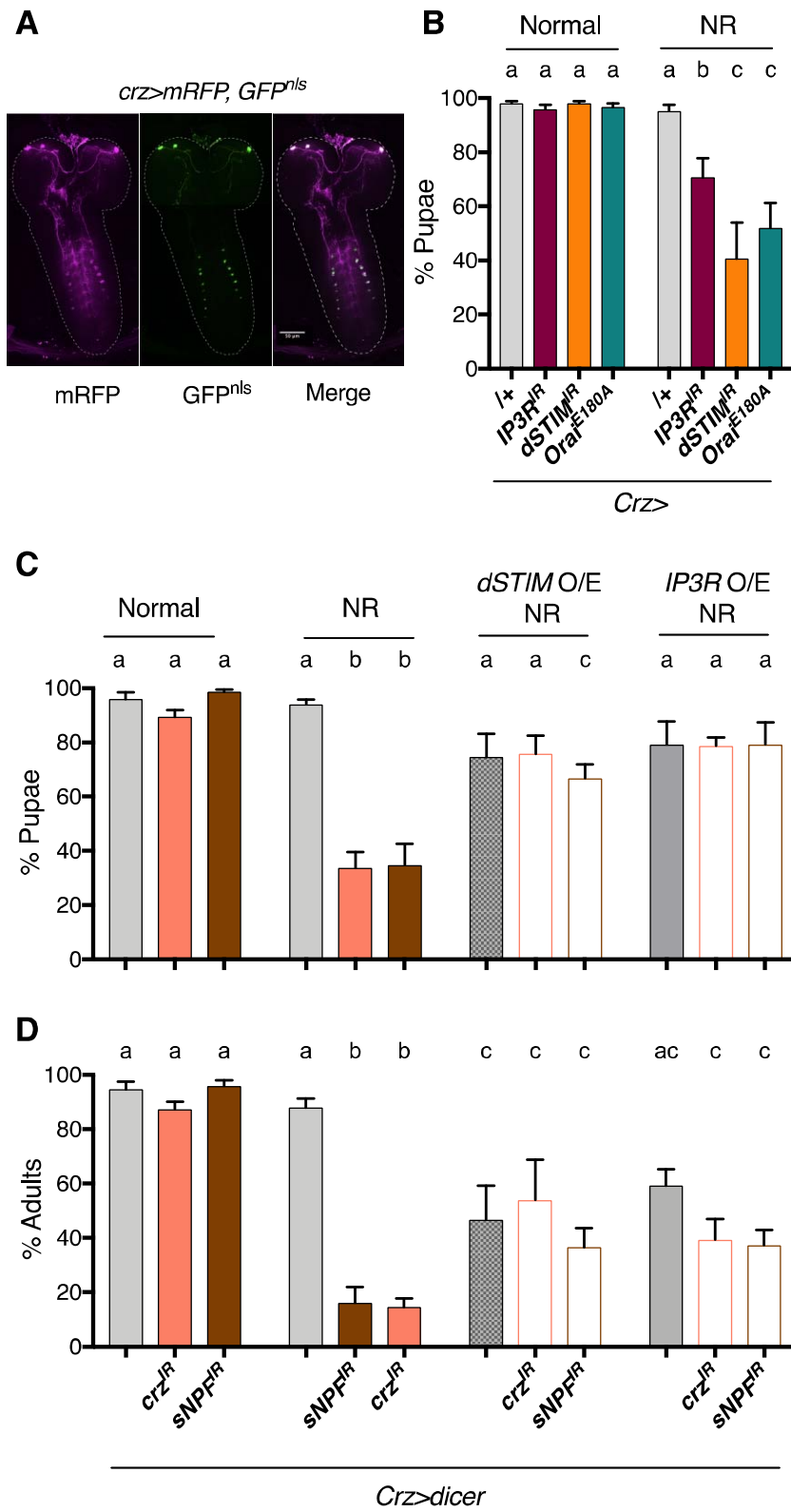
124 To test if both sNPF and Crz were required, they were specifically reduced (*sNPF^{IR}*;
125 *Crz^{IR}*) in Crz neurons. Knockdown of either NP resulted in larvae with a pupariation defect
126 on NR media but not, on normal food (Fig. 1C; Fig. S1D). In *Drosophila* neurons, enhancing
127 the expression of SOCE regulators leads to increased SOCE [16]. To test the positive effect

128 of SOCE on Crz and sNPF, a genetic compensation experiment was carried out. The SOCE-
129 regulators, *IP₃R* or *dSTIM* were over-expressed in Crz neurons which also expressed reduced
130 levels of either sNPF or Crz. NR larvae with this genetic make-up showed a significant
131 improvement in pupariation on NR media, as compared to NR larvae with only reduced NPs
132 (Fig. 1C). Interestingly, the compensation was sufficient to also increase the number of
133 adults that emerged (Fig. 1D). Notably, over-expression of either of the two SOCE
134 molecules, *dSTIM* and *IP₃R* on their own, did not affect pupariation on either normal or NR
135 media (Fig. 1C), but unlike on normal food (Fig. S1E), did reduce development to adulthood
136 on NR media (Fig. 1D). These data underscore the sensitivity of Crz neurons to ER-Ca²⁺
137 homeostasis during NR.

138 Loss of *IP₃R* and sNPF has previously been shown to affect larval feeding [27–29].
139 Hence, larval intake of dye-colored food in a 2-hour span was measured. Age-synchronized
140 larvae with knockdown of either *dSTIM*, *IP₃R*, *Crz* or *sNPF* in Crz neurons exhibited no
141 difference in the amount of dye ingested (Fig. S1F), suggesting that developmental defects
142 in the NR assay do not arise from a fundamental feeding problem.

143 Altogether, these genetic experiments helped identify a set of NP expressing
144 neurons, the Crz neurons, a subset of which also express sNPF, in which SOCE plays an
145 important role during development on NR.

Figure 1



147 **Fig. 1 SOCE is required in Crz neurons for larval development on NR media. (A)**
148 Expression pattern of *Crz-GAL4* driver, used in this study to manipulate Crz neurons,
149 visualised by expressing membrane bound RFP (mRFP) and GFP with a nuclear localisation
150 signal (GFP^{nls}) **(B)** % Pupae upon reduction of SOCE by knockdown of *STIM* (*STIM^{IR}*), *IP₃R*
151 (*IP₃R^R*) or ectopic expression of a dominant-negative *Orai* (*Orai^{E180A}*) in Crz neurons. To
152 measure pupariation, twenty five, 88h±3h old larvae, per vial, were transferred to either
153 normal food (corn flour, yeast, sugar) (See materials and methods for exact composition) or
154 nutrient restricted (NR; 100mM Sucrose) media and number of pupae (and adults where
155 relevant) that developed were counted. N = 6 vials for all experiments in this study. **(C)** %
156 Pupae upon reduction of either *sNPF* or *Crz* (*Crz^{IR}*, *sNPF^{IR}*) in Crz neurons, and when, *dSTIM*
157 or *IP₃R* are expressed in this background (*dSTIM* O/E; *IP₃R* O/E). **(D)** % Adults recovered for
158 genotypes in **(C)**. Bars with the same alphabet represent statistically indistinguishable
159 groups. Two-way ANOVA with Sidak multi comparison $p < 0.05$ for (B), (C) and (D). See
160 also Figure Supplement 1.
161

162 **Crz⁺ and sNPF⁺ DLP neurons majorly contribute to development on NR, and are**
163 **activated by NR**

164 In the larval CNS, Crz is expressed in 3 pairs of DLPs (Dorso Lateral Peptidergic
165 neurons) in the *pars lateralis* region of the brain lobes, 1 pair of neurons in dorso-medial
166 region and 8 pairs of interneurons in the VG (ventral ganglion) [30]. Other than the dorso-
167 medial neurons, the *Crz-GAL4* used in this study recapitulates the known expression
168 pattern for Crz. (Fig. S2A, B; Cartoon: Fig. 2A). Additionally, adjacent to DLPs, low
169 expression of *Crz-GAL4* was observed in 3-4 neurons that do not express Crz (Fig. S2A and
170 Fig. S2C). As mentioned previously, Crz⁺ DLPs co-express sNPF [24]. In terms of neuronal
171 architecture, the DLP neurons have two major branches: the anterior branch culminates in
172 a dense nest of neurites at the ring gland (RG), while the posterior branch terminates in the
173 subesophageal zone (SEZ). The VG neurons form a network amongst themselves to
174 ultimately give rise to two parallel bundles that travel anteriorly, and end in the brain lobes.
175 To visualize the overall distribution of NPs in the Crz neurons, we ectopically expressed a
176 rat neuropeptide coupled to GFP (ANF::GFP), a popular tool used to track NP transport and
177 release in *Drosophila* [31] (Fig. S2D). Firstly, within the DLPs, like Crz::mcherry (Fig. S2A),
178 ANF::GFP was either in the cell bodies or RG projections, but not in the projections
179 terminating at the subesophageal zone (Fig. S2D), suggesting selective NP transport to the
180 RG, which is a major neurohaemal site for systemic release of neuropeptides. Secondly,
181 ANF::GFP intensity was higher in the cell bodies of the DLPs than VG neurons (Fig. S2D).

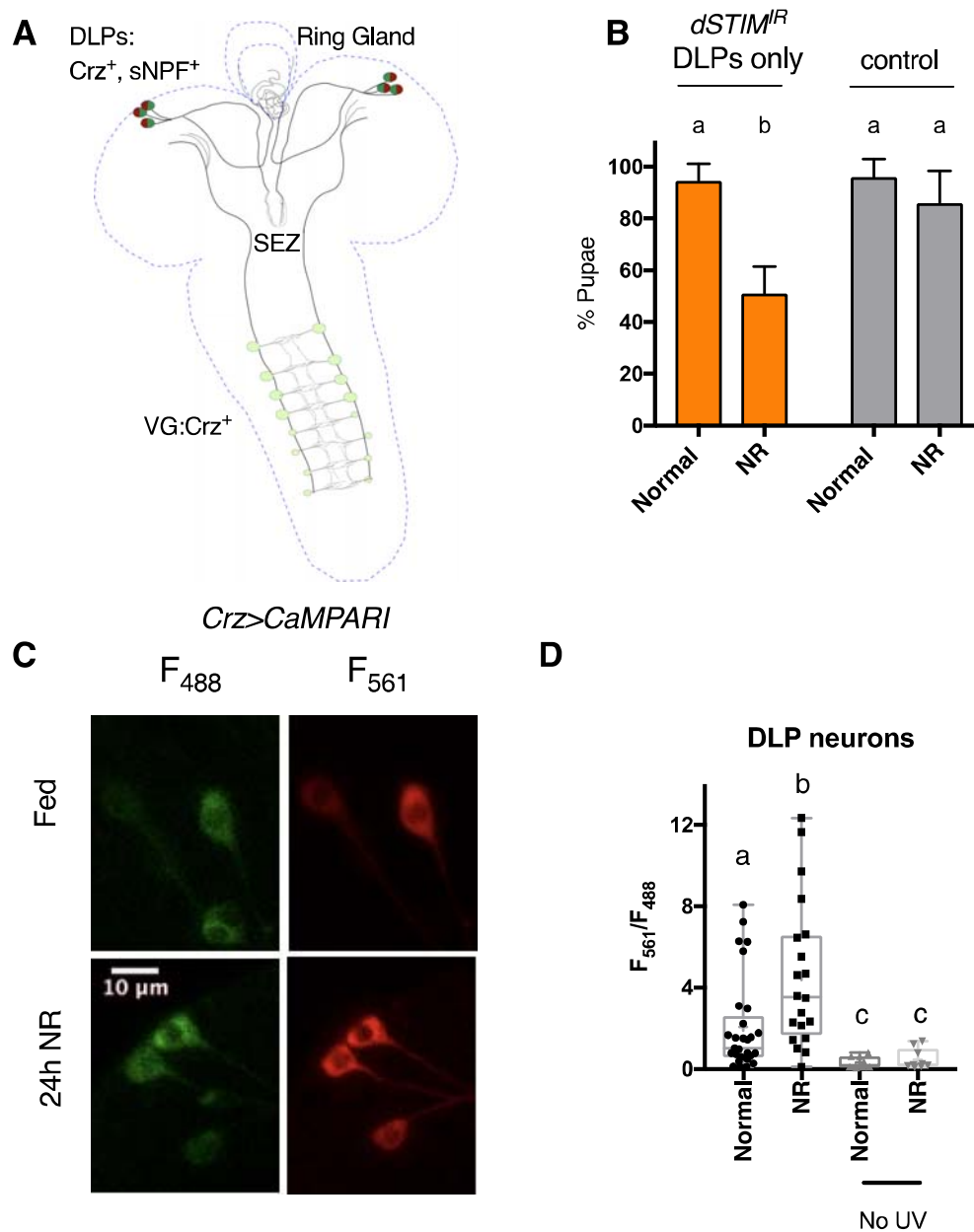
182 The close proximity of the terminal projections of the Crz⁺ VG neurons and the
183 anterior branch of the Crz⁺ DLP neurons in the brain lobe suggested possible
184 neuromodulation between the two sets of neurons. Therefore, we undertook experiments
185 to distinguish the contribution of DLPs vs VG localized Crz neurons, to the development in

186 NR media. First, we utilized *tshGAL80* to restrict *Crz-GAL4* expression to the DLPs (Fig.
187 S2E). The level of pupariation under NR conditions observed with restricted expression of
188 *dSTIM^{IR}* (Fig. 2B; Mean: 51%±4.2) was similar to that seen with full expression (Fig. 1B;
189 Mean: 40.7%±13.3), suggesting a major contribution of the DLP neurons to the NR
190 phenotype. Furthermore, *sNPF>Crz^{IR}* larvae have levels of pupariation of NR larvae (Fig.
191 S2F; Mean: 30.9%±7.8) similar to *Crz>Crz^{IR}* NR larvae (Fig. 1C; Mean: 33.8%±5.9). Because
192 *sNPF-GAL4* marks only the *Crz⁺* DLP neurons and not the *Crz⁺* VG neurons (Fig. S1C), this
193 too suggests a major role for the *Crz⁺* DLP neurons.

194 Requirement of SOCE in *Crz* neurons for pupariation on NR (Fig. 1C) suggested that
195 these neurons experience elevated cytosolic Ca^{2+} in NR conditions and are therefore,
196 stimulated by chronic starvation. To test this, the UV light-activated genetically encoded
197 calcium sensor, CaMPARI [32], was utilised. The sensor fluoresces in the GFP range (F_{488})
198 and is converted irreversibly to fluoresce in the RFP range (F_{561}), when exposed to UV light
199 and in the presence of Ca^{2+} . The level of conversion positively titrates with Ca^{2+}
200 concentrations. Larva expressing CaMPARI in *Crz⁺* neurons were placed in either normal or
201 NR media for 24 hours (24h NR). Whole larvae were immobilized, and exposed to UV light
202 for 2mins. Control larva were subject to the same treatment but, without being exposed to
203 UV light (Fig. 2C,D; no UV). Detection of F_{561} in the fed state suggests that these neurons
204 are active even under normal food conditions (Fig. 2C,D). Notably, after 24 hours on NR
205 media, chronic starvation caused a ~2-fold increase in average levels F_{561} and therefore, of
206 neuronal activation (Fig. 2D). F_{561}/F_{488} ratios did not appear to change in the VG neurons
207 (Fig. S2G,H). While there is a possibility that VG neurons do not exhibit higher F_{561} because
208 of insufficient penetration of UV light, the CaMPARI results together with the genetic

209 experiments (Fig. 2B, S2F), formed the basis for selecting the DLP neurons for further
 210 analysis on how dSTIM affects Crz and sNPF.
 211

Figure 2



212

213 Fig. 2 Crz⁺ and sNPF⁺ DLPs are required for development on NR media and activated by

214 NR (A) Cartoon of Crz⁺ and sNPF⁺ neurons in the larval CNS marked by *Crz-GAL4*. DLP:

215 dorso lateral peptidergic; VG: Ventral Ganglion; SEZ: Subesophageal zone **(B)** % Pupae
216 when *dSTIM* is selectively down-regulated only in Crz⁺ and sNPF⁺ DLPs, by using the *tsh*-
217 *Gal80* transgene and in the presence of *dicer2*. Control: *tshGal80/+;dSTIM^{IR}/+* . Data
218 represents mean ± SEM **(C)** Representative image. Expression of the UV-activated Ca²⁺
219 indicator, CaMPARI in Crz⁺ and sNPF⁺ DLPs, in larvae on 24 hours of normal (Fed) or NR
220 media (24h NR). Fluorescence at 561nm (F₅₆₁) reflects Ca²⁺ levels, while at 488nm (F₄₈₈)
221 reflects levels of the indicator CaMPARI. **(D)** Quantification of Ca²⁺ levels as reported by
222 F_{561/488} ratio in DLPs in larvae on 24 hours of normal or NR media, in the presence and
223 absence of UV-stimulation. N>7 larvae for UV-stimulated; N=3 for No UV stimulation. Bars
224 with the same alphabet represent statistically indistinguishable groups. Two-way ANOVA
225 with Sidak multi comparison test p<0.05 for (B). Mann-Whitney Test for (D). See also Figure
226 Supplement 2.

227 ***dSTIM* regulates NP synthesis and release in Crz neurons**

228 Crz peptide levels were measured in DLP neurons by staining larval brains with an
229 antiserum raised against the mature Crz peptide sequence [33]. Two locations on the DLP
230 neurons were chosen for measurement: neuronal cell body/soma and neurite projections
231 on the RG. In control DLP neurons, 24 hrs of NR caused average levels of Crz levels to
232 increase, in both locations (Fig. 3A, S3A,B). In comparison, DLP neurons expressing *dSTIM^{IR}*
233 displayed increased Crz peptide levels on normal food itself, and this remained unaltered
234 upon NR, for both locations (Fig. 3A, S3B, C). sNPF levels could not be similarly measured
235 by immunofluorescence because sNPF is expressed in many neurons close to the DLPs (Fig.
236 S1C), making measurements specifically from the DLP soma difficult to quantify. Instead,
237 semi-quantitative, direct, mass spectrometric profiling of dissected RGs was employed.
238 This technique can measure peptide levels relative to stable isotopic standards at single
239 neurohaemal release sites [34]. As Crz levels between the cell bodies and projections
240 correlated, and Crz⁺ DLPs are the sole contributors of sNPF on the RG [24], this technique
241 allowed us to infer sNPF levels in DLPs. In controls, 24hrs of NR, increased the average level
242 of sNPF ~5-fold on the RG (Fig. 3C). In comparison, RG preparations from larvae where
243 DLPs express *dSTIM^{IR}*, displayed increased sNPF levels on normal food itself, and this
244 remained unaltered upon NR (Fig. 3C). Although Crz was detected in the RG preparations, it
245 was of much lower intensity. Average Crz levels increased with NR in the control, and in
246 *dSTIM^{IR}* condition, but statistically higher levels of Crz were seen only in the NR, *dSTIM^{IR}*
247 condition (Fig. S3E). Nonetheless, broad agreement in trends, between Crz using
248 immunofluorescence and sNPF using MALDI-MS, suggest that the two peptides are
249 similarly regulated by NR and *dSTIM*. This is consistent with genetic experiments which

250 showed that over-expression of *dSTIM* can rescue loss of both, sNPF as well as Crz (Fig.
251 1C,D).

252 Thus, increased activation of DLP neurons by NR (Fig. 2D), appears to result in
253 peptide accumulation. Loss of *dSTIM* increases peptide levels on normal food, and prevents
254 an increase in peptide levels upon NR.

255 As an ER-Ca²⁺ sensor, *dSTIM* may potentially regulate several cellular processes that
256 would affect NPs such as their synthesis, processing, trafficking and/or release. As *STIM*^{IR}
257 increased peptide levels in the cell body as well as neurite projections on the RG, a major
258 trafficking defect was unlikely (Fig. 3A vs S3B,C). This does not rule out a role for *dSTIM* in
259 dense-core vesicle trafficking, but merely indicates that trafficking of Crz is not observably
260 disrupted by *STIM*^{IR}. We therefore proceeded to examine systemic and cellular phenotypes
261 when molecules known to reduce overall NP synthesis (*InR*^{IR}; Insulin Receptor) [35], peptide
262 processing (*amon*^{IR}) [25], and vesicle exocytosis (*Ral*^{DN}) [17] were expressed in Crz neurons.
263 All three perturbations caused a pupariation defect on NR media (Fig. 3D). However,
264 despite similar systemic outcomes, *amon*^{IR}, which reduces the prohormone convertase
265 required for peptide maturation, reduced Crz levels (Fig. 3E). Because this is not seen with
266 *STIM*^{IR}, a role for *dSTIM* in peptide processing was not pursued further.

267 Expression of *InR*^{IR} caused a modest increase in Crz peptide levels in DLP neurons in
268 the fed state and peptide levels did not increase as in the control, in NR media (Fig. 3F). *InR*
269 is a global protein synthesis regulator, and its expression scales DIMM⁺ NE cell size, with
270 functional consequences [35]. As the Crz⁺ DLPs are DIMM⁺ [36], we expected *InR*^{IR} to
271 reduce, not increase peptide levels. A potential explanation for this observation is that Crz
272 peptide levels are under feedback regulation, which was substantiated when we examined
273 how Crz transcript and peptide levels are connected. Similarities between *InR*^{IR} and *STIM*^{IR}

274 phenotypes, coupled with a previous observation that IP₃R, another SOCE component,
275 positively regulates protein synthesis in *Drosophila* neuroendocrine cells [22], prompted us
276 to test if *dSTIM* too regulates protein synthesis in general. We ectopically expressed a
277 physiologically irrelevant neuropeptide construct (ANF::GFP), that yields a processed
278 peptide in *Drosophila* neurons [31]. ANF::GFP levels in control and *dSTIM*^{IR} DLP neurons
279 were similar (Fig. S3E), suggesting that *dSTIM* does not have generic effects on peptide
280 synthesis. Instead, its effect on Crz and sNPF synthesis may be specific. The lack of Crz
281 elevation upon NR, in DLP neurons where *InR*^{IR} is expressed, leads to the speculation that
282 InR signalling is required for the up-regulation of protein synthesis needed for increased
283 peptide synthesis, processing and packaging during NR.

284 We previously found that *Ral* expression lies downstream of *dSTIM*-mediated SOCE
285 in *Drosophila* pupal brains [37], and in dopaminergic neurons, over-expression of *Ral*^{DN}
286 reduces secretion of ANF::GFP [17]. These previous data, coupled with the observation that
287 *Ral*^{DN} and *dSTIM*^{IR} show similarly high Crz levels in the fed state, suggest that *dSTIM* affects
288 vesicle secretion through regulation of *Ral* expression. To independently validate if vesicle
289 release is important in Crz neurons, we over-expressed a temperature sensitive dynamin
290 mutant (*Shibire*^{ts}) also shown to reduce NP release [38] and tetanus toxin (*TNT*) shown to
291 prevent release of eclosion hormone, a neuropeptide [39]. Both manipulations caused a
292 pupariation defect on NR (Fig. S3F). It is unclear why *Ral*^{DN} causes Crz levels to decrease
293 upon NR. In *Drosophila* pacemaker neurons, *Ral* has been shown to bias the sensitivity of a
294 neuropeptide receptor, the Pigment Dispensing Factor Receptor [40]. Perhaps, functions
295 distinct from *Ral*'s contribution to vesicle exocytosis contribute to this observation.
296 Nonetheless, the lack of increase in Crz levels in DLP neurons upon NR, when *InR*^{IR} and
297 *Ral*^{DN} are expressed, assumes significance in the context of pupariation of NR larvae.

298 Control larvae subject to 24hrs of NR, display increased Crz (Fig. 3A) and sNPF (Fig. 3C)
299 levels, and then proceed to successfully complete development to pupae (Fig. 1C).
300 Whereas, in *dSTIM^{IR}*, *InR^{IR}* and *Ral^{DN}* conditions, on NR, neither do DLPs display increased
301 Crz levels (Fig. 3A, 3F), nor do all larvae pupariate (Fig. 1B, 1C, 3D). Thus, an increase in
302 peptide levels on NR correlates with larval ability to pupariate on NR. Taken in context with
303 increased neuronal activation during NR (Fig. 2D), and evidence that functional vesicle
304 exocytosis (Fig. 3D, S3F) as well as adequate peptide production (Fig. 3D) is required for
305 survival on NR, these data suggest that increased production and release of Crz and sNPF
306 during NR, is required for NR larvae to successfully complete development.

307 To prove that Crz and sNPF are released during NR, the ideal experiment would be
308 to measure levels of secreted NPs. But small size (8-10 amino acids), low hemolymph titres
309 and high complexity of hemolymph, make peptide measurements by biochemical means
310 highly challenging in *Drosophila*. Moreover, NPs exhibit endocrine as well as paracrine
311 signalling [41]; and the latter will not be reflected in hemolymph measurements.
312 Fortunately, in the Crz signalling system there is feedback compensation between secreted
313 Crz and Corazonin receptor (*CrzR*) mRNA levels, providing a means to gauge secreted Crz
314 levels indirectly. In adults, expression of *Crz^{IR}* in Crz neurons, increased levels of *CrzR* on the
315 fat body [42]. We thus tested if *CrzR*, which in larvae appears to be expressed in the salivary
316 glands and CNS [43], was subject to similar feedback. In larval brains, reducing Crz, using
317 two different *Crz^{IR}* strains, not only caused a reduction in *Crz* mRNA levels (Fig. 3G), but also
318 a concomitant increase in *CrzR* mRNA levels (Fig. 3H). Conversely, reducing *CrzR* levels
319 (*CrzR^{IR}*) in the larval CNS, results in up-regulation of *Crz* mRNA (Fig. S3G). This confirmed
320 the existence of feedback in the Crz signalling system, and the use of neuronal *CrzR*
321 transcript levels as a measure of secreted Crz levels. In line with this inference, we observed

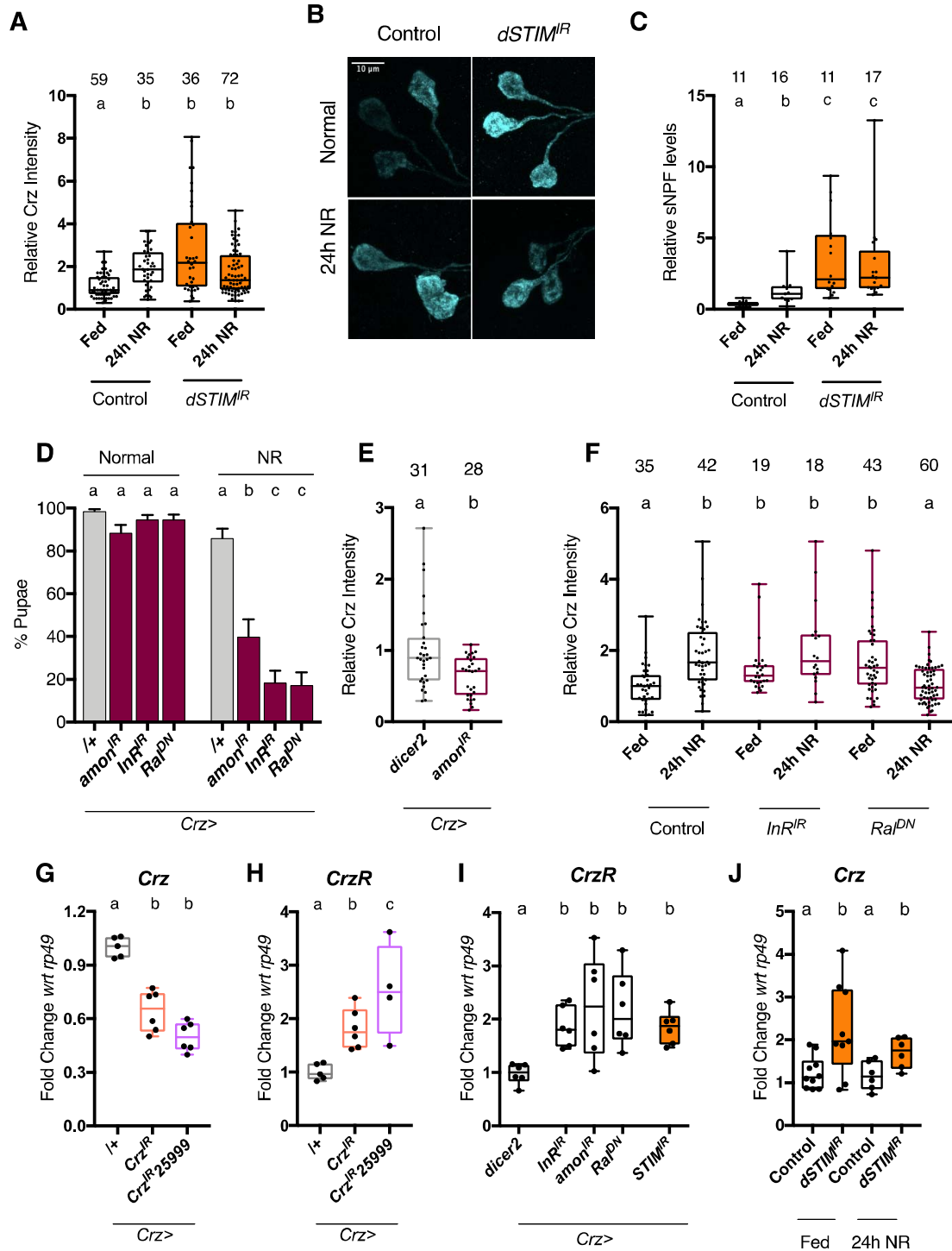
322 an up-regulation of *CrzR* mRNA in larval brains where *Crz* neurons are expressing either
323 *InR^{IR}* or *amon^{IR}* or *Ral^{DN}* (Fig. 3I). Therefore, the observation that in the *STIM^{IR}* condition
324 *CrzR* mRNA levels are high (Fig. 3I), supports the idea that dSTIM function is necessary for
325 the secretion of optimal levels of *Crz*.

326 Because dSTIM-mediated SOCE is known to induce changes in gene expression [37],
327 we probed if *Crz* expression is sensitive to NR and *dSTIM*. In the control, NR did not change
328 *Crz* mRNA levels (Fig. 3J), suggesting that a post-transcriptional mechanism is responsible
329 for increasing *Crz* peptide levels upon NR (Fig. 3A,S3B,C). In the *STIM^{IR}* condition, *Crz*
330 transcript levels were up-regulated on normal food conditions (Fed) and no further increase
331 was observed upon NR (Fig. 3J). The straightforward explanation for high *Crz* peptide levels
332 in *STIM^{IR}* condition could therefore be attributed to higher gene expression of *Crz*.

333 However, data from other perturbations in *Crz* neurons suggested that a linear
334 interpretation between *Crz* mRNA and peptide levels cannot not be made. When *Crz^{IR}* is
335 expressed, *Crz* mRNA is reduced (Fig. 3G), but peptide levels are elevated (Fig. S3I);
336 whereas, when *amon^{IR}* is expressed, *Crz* mRNA is increased (Fig. S3H), but peptide levels
337 are decreased (Fig. 3E). Meanwhile, in three conditions, *Crz* mRNA as well as peptide levels
338 are higher than controls: *Crz^R* (Fig. S3G vs S3I), *InR^{IR}* (Fig. S3H vs Fig. 3F) and *Ral^{DN}* (Fig.
339 S3H vs Fig 3F). Note also that both higher (*dSTIM^{IR}*, *InR^{IR}*, *Ral^{DN}*) or lower (*amon^{IR}*) *Crz*
340 peptide levels in DLP cell bodies, result in reduced systemic *Crz* signalling (*CrzR* mRNA
341 levels; Fig. 3I). These data indicate that *Crz* transcription, translation and release are
342 independently regulated. A simple explanation for elevated levels of *Crz* transcript as well
343 as peptide levels in *STIM^{IR}* is therefore, feedback compensation. Moreover, there is no
344 change in *Crz* mRNA upon 24hrs of NR, when *STIM^{IR}* is expressed (Fig. 3J). Together, this
345 argues against a direct role for *dSTIM* in regulating *Crz* gene expression.

346 In summation, these data have been inferred as follows: on normal food, partial loss
347 of *dSTIM* reduces systemic Crz signalling, indicating a requirement for *dSTIM* in Crz
348 secretion. On NR media, Crz⁺ DLPs are stimulated to increase peptide synthesis and
349 release, in order for NR larvae to complete development. Peptide up-regulation upon NR is
350 abrogated when *dSTIM* is reduced. These add up to suggest that *dSTIM* compromises NE
351 cell function in a manner that affects peptide synthesis and release, with functional
352 consequences for survival on NR.

Figure 3



353

354 **Fig 3. *dSTIM* regulates *Crz* and sNPF levels.** Larvae were subjected to 24 hours of normal
355 (fed) or nutrient restricted (NR) media. *Crz* levels were measured in DLP neurons by

356 immunofluorescence on larval brains. All manipulations were performed using the *Crz-*
357 *GAL4* driver **(A)** Relative levels of Crz peptide in DLP neuron cell bodies, Control=*crz>dicer2*
358 *. dSTIM^{IR}=crz>dSTIM^{IR},dicer2*. Number of cells measured shown atop bars. N>12 brains **(B)**
359 Representative images for cell bodies measured in (A). **(C)** Relative levels of total sNPF
360 peptides measured on dissected ring glands (N atop bars) and quantified using MALDI-MS.
361 Externally added heavy standard (Hug-PK*) was used to normalise peptide levels between
362 samples. **(D)** % Pupae on normal or NR media, upon reduced peptide processing
363 (*amon^{IR},dicer2*) protein synthesis (Insulin receptor; *InR^{IR}*) or vesicle exocytosis (dominant-
364 negative *Ral*; *Ral^{DN}*) in *Crz⁺* neurons. Data represents mean \pm SEM **(E)** Relative levels of Crz
365 upon expression of *amon^{IR}* and *dicer2*. N>10 brains. **(F)** Relative levels of Crz upon indicated
366 cellular perturbation of *Crz⁺* neurons. N \geq 6 brains. control: *Crz-GAL4/+*. **(G)** *Crz* mRNA levels
367 from larval brains when *Crz* is reduced by two different RNAi lines. N \geq 5. **(H)** Corazonin
368 receptor (*CrzR*) mRNA levels from larval brains with reduced *Crz*. N \geq 4. **(I)** *CrzR* mRNA
369 levels from larval brains expressing indicated cellular perturbations in *Crz* neurons. N \geq 6 **(J)**
370 *Crz* mRNA levels from larval brains. Control=*crz>dicer2* *. dSTIM^{IR}=crz>dSTIM^{IR},dicer2* N \geq 6.
371 Bars with the same alphabet represent statistically indistinguishable groups. Kruskal-Wallis
372 Test with Dunn's multicomparison correction $p < 0.05$ for (A), (C), (F). Mann-Whitney Test
373 for (E). Two-way ANOVA with Sidak's multi comparison test $p < 0.05$ for (D), (J). One-way
374 ANOVA with Tukey multi comparison test $p < 0.05$ for (G), (H), (I). See also Figure
375 Supplement 3.

376
377 **Systemic and cellular phenotypes observed with reduced *dSTIM* in Crz neurons can be**
378 **rescued by increasing synthesis and release of peptides**

379 To validate a role for dSTIM in peptide synthesis and release, we tested genetic
380 perturbations that can compensate for this deficiency, to rescue developmental and cellular
381 phenotypes associated with *dSTIM^{IR}* expression in Crz neurons. In the case of NPs, genetic
382 over-expression may not translate to enhanced release, as proteins involved in NP
383 processing as well as the regulated secretory pathway would need to be up-regulated.
384 Furthermore, regulatory feedback from peptides to their transcription may complicate
385 over-expression, as seen for the Crz signalling system (Fig. S3I). To get around these issues,
386 and because *InR^{IR}* phenocopied *STIM^{IR}* (Fig. 3A,D,F,I, S3H), we opted to increase protein
387 synthesis by over-expression of the Insulin receptor (*InR*). Cell size (Fig. S4A) as well as Crz
388 levels (Fig. S4B,C) in DLP neurons scaled with *InR* over-expression, supporting the
389 effectiveness of *InR*. To increase release, we over-expressed *Ral^{WT}* as *Ral* over-expression
390 can compensate for vesicle release in dopaminergic neurons expressing *STIM^{IR}* [17]. In Crz
391 neurons with reduced *dSTIM*, over-expression of either *InR* or *Ral^{WT}* rescued pupariation on
392 NR media (Fig. 4A); restored peptide up-regulation upon NR (Fig. 4A,B) and decreased *CrzR*
393 mRNA back to control levels (Fig. 4D). Of note, over-expressing *Ral^{WT}* or *InR* by itself, in Crz
394 neurons, did not alter *CrzR* mRNA levels (Fig. 4D), suggesting that neuronal activation,
395 which happens on NR media (Fig. 2D) potentiates their activity.

396 To increase neuronal activity, we utilised the temperature and voltage-gated cation
397 channel, *TrpA1* [44]. Over-expression of *dTrpA1* and its activation by raising the
398 temperature to 30°C for 24 hours, in the *dSTIM^{IR}* background, rescued pupariation of NR
399 larvae (Fig. 4E). It also restored the ability of DLP neurons to increase Crz levels upon NR

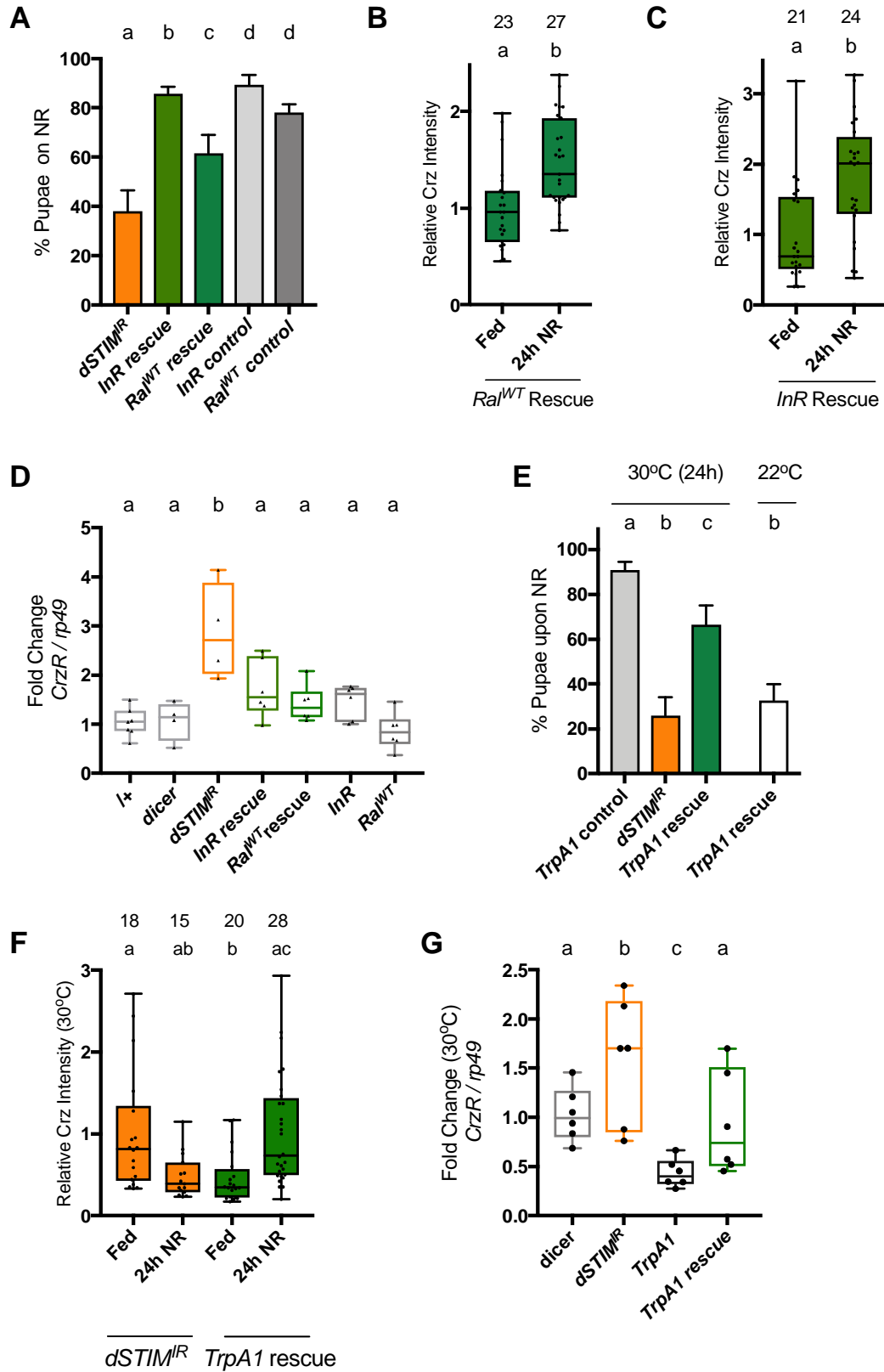
400 (Fig. 4F) and decreased levels of *CrzR* mRNA (Fig. 4G). In line with the feedback between
401 *CrzR* mRNA levels and systemic Crz signaling, over-expression of *dTrpA1* alone in Crz
402 neurons resulted in a decrease in *CrzR* mRNA levels (Fig. 4G), supporting the role for
403 neuronal activation in secreting Crz. Interestingly, development to adulthood on NR, for
404 *dSTIM^R* larvae, was also significantly increased upon over-expression of *InR* (Fig. S4E) and
405 *TrpA1* (Fig. S4F), but not *Ral^{WT}* (Fig. S4E).

406 An optogenetic approach, utilizing the over-expression of Channelrhodopsin (*ChR2-*
407 *XXL*), a light-sensitive cation channel, also rescued pupariation but not to the same extent
408 (Fig. S4D). Poorer rescue with *ChR2-XXL* could be because sustained activation of this
409 channel depress synaptic transmission and the channel is less conductive for Ca^{2+} compared
410 to *TrpA1* [45]. Similar genetic manipulation, with *TrpA1* and *ChR2-XXL*, in a hypomorphic
411 IP_3R mutant (*itpr^{ku}*) resulted in a small but significant rescue of *itpr^{ku}* pupariation on NR
412 media (Fig. S4G,H).

413 Together, these results strongly suggested that defects arising from dysregulated
414 intracellular Ca^{2+} signalling, may be overcome by increasing vesicle exocytosis (*Ral^{WT}*,
415 *TrpA1*, *ChR2-XXL rescue*) or protein synthesis (*InR rescue*). Importantly, the rescues
416 observed with *InR*, *Ral^{WT}* and *dTrpA1* are effective at the molecular (*CrzR* levels), cellular
417 (Crz peptide levels upon NR) as well as systemic (NR larvae) level.

418

Figure 4



420 **Fig 4. Systemic and cellular phenotypes caused by partial loss of dSTIM in Crz neurons,**
421 **can be rescued by increasing peptide synthesis or release. (A)** % Pupae upon expression
422 of Insulin receptor (*InR*) or Ral (*Ral^{WT}*) in Crz neurons expressing *dSTIM^{IR}*. Genotypes:
423 *dSTIM^{IR} = crz>dSTIM^{IR}*. *InR* rescue=*Crz>InR,dSTIM^{IR},dicer2*. *Ral^{WT}* rescue=*Crz>Ral^{WT},*
424 *dSTIM^{IR},dicer2*. *InR* control: *dicer2;InR/+; dSTIM^{IR} /+;* *Ral^{WT}* control: *Ral^{WT} /+; dSTIM^{IR} /+.* Data
425 represents mean ± SEM. **(B)** *Ral^{WT}* rescue or **(C)** *InR* rescue larvae were transferred to
426 normal (Fed) or NR media for 24 hours. Crz immunofluorescence levels in DLP neurons
427 were measured. Number of cells measured shown atop bars. N>7 brains **(D)** *Crz* receptor
428 (*CrzR*) mRNA levels in larval brains expressing various molecules in Crz neurons.
429 *InR=Crz>InR*. *Ral^{WT}=Crz>Ral^{WT}*. N≥4. **(E)** % Pupae upon expression of TrpA1 in Crz neurons
430 expressing *dSTIM^{IR}*. TrpA1 control: *dicer2;TrpA1/+; dSTIM^{IR} /+;* TrpA1 rescue: *Crz>TrpA1,*
431 *dSTIM^{IR},dicer2*. Larvae were reared at 25°C, at 88h±3h AEL age transferred to NR media and
432 incubated either at 30°C or 22°C for 24 hours, and returned to 25°C thereafter. Data
433 represents mean ± SEM. **(F)** Crz levels in DLP neurons upon 24 hrs of NR or normal food
434 (Fed) at 30°C for indicated genotypes. N > 5 brains. **(G)** *Crz* receptor (*CrzR*) transcript levels
435 in larval brains expressing various molecules in Crz⁺ neurons, when larvae are reared at
436 30°C. TrpA1: *Crz>TrpA1*. N=6. one-way ANOVA with a post hoc Tukey's test p<0.05 for (A),
437 (D), (E), (G). Mann-Whitney test for (B), (C). Kruskal-Wallis Test with Dunn's multi-
438 comparison correction p<0.05 for (F). See also Figure Supplement 4.
439

440 Discussion

441 This study employed an *in vivo* approach coupled to a functional outcome, in order
442 to broaden our understanding of how STIM regulates neuropeptides. A role for dSTIM-
443 mediated SOCE in *Drosophila* neuroendocrine cells for survival on NR was previously
444 established [22]. The previous study offered the opportunity to identify SOCE-regulated
445 peptides, produced in these neuroendocrine cells, that could be investigated in a
446 physiologically relevant context.

447 In *Drosophila*, both Crz and sNPF have previously been attributed roles in many
448 different behaviours. Crz has roles in adult metabolism and stress responses [42,46–48],
449 sperm transfer and copulation [49], and regulation of ethanol sedation [50,51]. While, sNPF
450 has been implicated in various processes including insulin regulation (Kapan et al., 2012;
451 Lee et al., 2008) circadian behaviour [53], sleeping [54,55] and feeding [27]. Thus, the
452 identification of Crz and sNPF in coping with nutritional stress is perhaps not surprising, but
453 a role for them in coordinating the larval to pupal transition under NR is novel.

454 A role for Crz in conveying nutritional status information was originally proposed by
455 Jan Veenstra [56], which this study now supports. In larvae, Crz⁺ DLPs are known to play a
456 role in sugar sensing [57] and in adults, they express the fructose receptor Gr43a [58].
457 Additionally, they express receptors for neuropeptides DH31 [59], DH44 [59] and AstA [56],
458 which are made in the gut as well as larval CNS. Together, these observations and our study
459 are strongly indicative of a role for Crz⁺ DLPs in directly or indirectly sensing nutrients, with
460 a functional role in larval survival and development in nutrient restricted conditions.

461 Several neuropeptides and their associated signalling systems are evolutionarily
462 conserved [11,12]. The similarities between Crz and GnRH (gonadotrophin-releasing
463 hormone), and sNPF and PrRP (Prolactin-releasing peptide), at the structural [11],

464 developmental [60] and receptor level therefore, is intriguing. Structural similarity of
465 course does not imply functional conservation, but notably, like sNPF, PrRP has roles in
466 stress response and appetite regulation [61]. This leads to the conjecture that GnRH and
467 PrRP might play a role in mammalian development during nutrient restriction.

468 dSTIM regulates Crz and sNPF at the levels of peptide release and likely, peptide
469 synthesis upon NR. We speculate that neuroendocrine cells can use these functions of
470 STIM, to fine tune the amount and timing of peptide release, especially under chronic
471 stimulation (such as 24hrs NR), which requires peptide release over a longer timeframe.
472 Temporal regulation of peptide release by dSTIM may also be important in neuroendocrine
473 cells that co-express peptides with multifunctional roles, as is the case for Crz and sNPF. It
474 is conceivable that such different functional outcomes may require distinct bouts of NP
475 release, varying from fast quantile release to slow secretion [62]. As elevation in cytosolic
476 Ca^{2+} drives NP vesicle release, neurons utilise various combinations of Ca^{2+} influx
477 mechanisms to tune NP release. For example, in *Drosophila* neuromuscular junction,
478 octopamine elicits NP release by a combination of cAMP signalling and ER-store Ca^{2+} , and
479 the release is independent of activity-dependent Ca^{2+} influx [63]. In the mammalian dorsal
480 root ganglion, VGCC activation causes a fast and complete release of NP vesicles, while
481 activation of TRPV1 causes a pulsed and prolonged release [64]. dSTIM-mediated SOCE
482 adds to the repertoire of mechanisms that can regulate cytosolic Ca^{2+} levels and therefore,
483 vesicle release. This has already been shown for *Drosophila* dopaminergic neurons [17] and
484 this study extends the scope of release to peptides. Notably, dSTIM regulates exocytosis
485 via Ral in neuroendocrine cells, like in dopaminergic neurons.

486 In *Drosophila* larval Crz⁺ DLPs, dSTIM appears to have a role in both fed, as well as
487 NR conditions. On normal food, not only do Crz⁺ DLPs exhibit small but significant levels of

488 neuronal activity (Fig. 2D) but also, loss of dSTIM in these neurons reduced Crz signalling
489 (Fig. 3I). Thus, dSTIM regulates Ca²⁺ dynamics and therefore, neuroendocrine activity,
490 under basal as well as stimulated conditions. This is consistent with observations that basal
491 SOCE contributes to spinogenesis, ER-Ca²⁺ dynamics as well as transcription [65].
492 However, in our case, this regulation appears to have functional significance only in NR
493 conditions as pupariation of larvae, with reduced levels of *dSTIM* in Crz⁺ neurons, is not
494 affected on normal food (Fig. 1B). In a broader context, STIM is a critical regulator of
495 cellular Ca²⁺ homeostasis as well as SOCE, and a role for it in the hypothalamus has been
496 poorly explored. Because STIM is highly conserved across the metazoan phyla, our study
497 predicts a role for STIM and STIM-mediated SOCE in peptidergic neurons of the
498 hypothalamus. There is growing evidence that SOCE is dysregulated in neurodegenerative
499 diseases [66]. In neurons derived from mouse models of familial Alzheimer's disease [67]
500 and early onset Parkinson's [65], reduced SOCE has been reported. How genetic mutations
501 responsible for these diseases manifest in neuroendocrine cells is unclear. If they were to
502 also reduce SOCE in peptidergic neurons, it's possible that physiological and behavioural
503 symptoms associated with these diseases, may in part stem from compromised SOCE-
504 mediated NP synthesis and release.

505 **Material and Methods**

506 **Fly Husbandry**

507 Flies were grown at 25°C in 12h:12h L:D cycle. Normal food: (1L recipe: 80g corn flour,
508 20g Glucose, 40g Sugar, 15g Yeast Extract, 4mL propionic acid, *p*-hydroxybenzoic
509 acid methyl ester in ethanol 5mL, 5mL ortho butyric acid) For nutritional stress assay,
510 flies were allowed to lay eggs for 6 hours on normal food. After 88hours, larvae were

511 collected and transferred to either normal or NR (100mM Sucrose) food. Pupae and adults
512 were scored after 10 days of observation.

513 **Fly strains.**

514 *Canton S* was used as the wild type (+) control.

515 The following strains were obtained from Bloomington Drosophila Stock Centre: *AKH-*
516 *GAL4* (25684), *Crz-GAL4* (51976), *DSK-GAL4* (51981), *sNPF-GAL4* (51981), *UAS-Crz^{IR}* 25999
517 (25999), *UAS-dicer2* (24651), *UAS-TeTxLc* (28837), *UAS-TeTxLc-IMP* (28838), *UAS-CaMPARI*
518 (58761), *UAS-GFP^{nls}* (4776), *UAS-mRFP* (32218), *UAS-TrpA1* (26263), *UAS-InR* (8248), *UAS-*
519 *amon^{IR}* (28583), *UAS-Ral^{DN}* (32094)

520 The following strains were obtained from Drosophila Genetic Resource Center, Kyoto:

521 *sNPF-GAL4* (113901)

522 The following were from Vienna Drosophila Research Centre stock collection: *UAS-IP₃R^{IR}*
523 (106982), *UAS-STIM^{IR}* (47073), *UAS-Crz^{IR}* (30670), *UAS-InR^{IR}* (999)

524 The following was from Exelixis at Harvard Medical School: *sNPF⁰⁰⁴⁴⁸* (00448)

525 The following were kind gifts: *AstA¹-GAL4* (David Anderson), *dILP2-GAL4* (Eric Rulifson),
526 *hug-GAL4* (Michael Pankratz), *NPF-GAL4* (Ping Shen), *UAS-sNPR^{IR}* (Kweon Yu),
527 *Crz::mCherry* (Gábor Juhász), *UAS-hid::UAS-rpr* (Tina Mukherjee), *UAS-Shibire^{ts}* (Toshihiro
528 Kitamoto), *tsh-GAL80* (Julie Simpson), *UAS-preproANF::GFP* (Edwin Levitan), *UAS-*
529 *ChR2XXL* (Robert Kittel and Georg Nagel)

530 The following were previously generated in our laboratory: *itpr^{ka1091}*, *itpr^{ug3}*, *UAS-Orai^{E180A}*,

531 *UAS-itpr⁺*, *UAS-Stim*, *UAS-Ral^{WT}*

532 **Larval Feeding**

533 Ten 3rd instar larvae were collected and placed on cotton wool soaked with solution of 4.5%
534 dissolved yeast granules and 0.5% Erioglucine (Sigma, 861146). Controls contained no

535 dye. Feeding was allowed for 2 hours at 25°C. 5 larvae per tube were crushed in 100µL of
536 double distilled water. Solution was spun at 14000 rpm for 15 minutes and 50µL was
537 withdrawn for absorbance measurement at 625nm in a 96-well plate. 5µL was used to
538 measure protein content using the Pierce BCA Protein Assay kit (#23227).

539 **qRT-PCR**

540 RNA was isolated from 12-15 larval brains at the specified time points using Trizol. cDNA
541 synthesis was carried out as described [26]. All mRNA levels are reported as fold change
542 normalized to *rp49*. Primer sequences:

543 *rp49*, F:CGGATCGATATGCTAAGCTGT, R:GCGCTTGTTTCGATCCGTA.

544 *Crz*, F:TCCTTTAACGCCGCATCTCC, R:CGTTGGAGCTGCGATAGACA

545 *CrzR*, F:CTGTGCATCCTGTTTGGCAC, R:GGCCTTGTGTATCAGCCTCT

546 **Measuring neuronal activation using CaMPARI**

547 Early third instar larvae were transferred to either normal or NR food. After 24 hours, larvae
548 were recovered and immobilized on double sided tape. UV light from a Hg-arc lamp was
549 focused using the UV filter, on the larvae through a 10X objective on Olympus BX60, for 2
550 minutes. Larvae were then immediately dissected in ice-cold PBS, mounted in PBS and
551 imaged using Olympus FV-3000 Confocal microscope using a 40X objective and high-
552 sensitivity detectors. Microscope settings for laser intensity, PMT settings and
553 magnification were kept identical for all measurements. Each experiment always had a no
554 UV control, in which larvae were subject to immobilisation but not UV light. Fluorescence
555 intensity was calculated for each cell body using Image J.

556 **Immunofluorescent staining**

557 For expression patterns, 3rd instar larval brains with RGs attached were dissected in ice-
558 cold PBS and fixed in 3.7% formaldehyde at 4°C for 20 mins. The samples were washed 4

559 times in PBS and mounted in 60% glycerol. Endogenous fluorescence was acquired on
560 Olympus FV-3000 using a 20X, 40X or 60X objective, and processed used ImageJ. For
561 samples requiring antibody staining brains were similarly processed and then subjected to
562 permeabilisation (0.3% Triton X-100 + PBS; PBSTx) for 15 mins, 4 hr blocking in 5% normal
563 goat serum in PBSTx at 40C, followed by overnight incubation in primary antibody (1:1000
564 Chicken-GFP, Abcam: ab13970) and secondary with Alexa 488 or Alexa 594 (1:400; Abcam).
565 For corazonin (1:1000; raised in Rabbit; Jan Veenstra, University of Bordeaux), all the above
566 steps remained the step, except that dissected brains were fixed for 1hr at RT in 4% PFA
567 and the secondary was anti-rabbit Alexa 405 (1:300, Abcam). Cell bodies were outlined
568 manually and integrated density was used to calculate CTCF (Corrected Total Cell
569 Fluorescence). For all samples, a similar area was measured for background fluorescence.

570 **Direct peptide-profiling by MALDI-TOF MS**

571 Ring glands were dissected in cold HL3.1 and transferred to a MALDI plate as previously
572 described [68]. 0.2 µl of matrix (saturated solution of recrystallized α-cyano-4-
573 hydroxycinnamic acid in MeOH/EtOH/water 30/30/40% v/v/v) was added, containing 10 nM
574 of stable isotope-labeled HUG-pyrokinnin (HUG-PK* (Ser-Val[d8]-Pro-Phe-Lys-Pro-Arg-
575 Leu-amide, Mw = 950.1 Da; Biosyntan, Berlin, Germany)) and 10 nM labeled
576 myosuppressin (MS* (Thr-Asp-Val[d8]-Asp-His-Val-Phe-Leu-Arg-Phe-amide, Mw =
577 1255.4 Da; Biosyntan) MALDI-TOF mass spectra were acquired in positive ion mode on a
578 4800 Plus MALDI TOF/TOF analyzer (MDS Sciex, Framingham, MA, USA) in a mass range
579 of 900-4000 Da and fixed laser intensity with 20 subspectra and 1000 shots per sample.
580 Data were analyzed with Data Explorer 4.10. Spectra were baseline corrected and de-
581 isotoped. The sum of the resulting relative intensities of the de-isotoped peaks was
582 calculated for the different ion adducts (H⁺, Na⁺, K⁺) of each peptide as well as the labeled

583 peptides*. Then, the ratios sNPF/HUG-PK* and corazonin/MS* were calculated, using the
584 labeled peptide with the most similar molecular weight. For sNPF, all isoforms (1/2-short, 1-
585 long, -3 and -4) variants were totaled.

586 **Optogenetic and thermogenic experiments**

587 For thermogenic (*dTrpA1*, *Shibire^{ts}*) experiments, larvae were matured to 88hours AEL at
588 25°C. After transfer to either NR or normal food, vials were placed at 22°C, 25°C or 30°C for
589 either 24 hours (*dTrpA1*) or till the end of observation time (*Shibire^{ts}*). For optogenetic
590 experiments (*Chr2-XXL*), larvae were matured to 88AEL in the dark. After transfer to either
591 NR or normal food, one set was placed in the dark while another was placed in an incubator
592 with regular white lights that were on continuously till the end of observation time.

593 **Author contributions**

594 M, C.W and G.H designed research; M performed research, except MALDI-MS which was
595 performed by C.W.; M, C.W and G.H. analysed data; M wrote the paper with inputs from
596 C.W. and G.H.

597 **Acknowledgments**

598 Supported by Wellcome Trust/ DBT India Alliance (Early Career Award #IA/E/12/1/500742 to
599 M) and NCBS core funding (GH). We thank Jan Veenstra for the Crz antibody and helpful
600 suggestions with immunostaining. Members of the Hasan lab for help with fly transfers,
601 critical comments and helpful discussions. Drosophila fly community (List in supplementary
602 information), BDSC, VDRC, NIG and DGRC for fly strains. NCBS Central Imaging and Flow
603 Facility, for imaging, and Jörg Kahnt (core facility for mass spectrometry and proteomics,
604 Max-Planck-Institute for Terrestrial Microbiology, Marburg) for access to the mass
605 spectrometer.

606 **Competing Interests**

607 All of the authors declare no financial and non-financial competing interests.

608 References

- 609 1. Prakriya M, Lewis RS. Store-Operated Calcium Channels. *Physiol Rev. United States;*
610 2015;95: 1383–1436. doi:10.1152/physrev.00020.2014
- 611 2. Putney JW, Steinckwich-Besançon N, Numaga-Tomita T, Davis FM, Desai PN,
612 D'Agostin DM, et al. The functions of store-operated calcium channels. *Biochim*
613 *Biophys Acta - Mol Cell Res.* 2017;1864: 900–906.
614 doi:<https://doi.org/10.1016/j.bbamcr.2016.11.028>
- 615 3. Brini M, Cali T, Ottolini D, Carafoli E. Neuronal calcium signaling: function and
616 dysfunction. *Cell Mol Life Sci. Switzerland;* 2014;71: 2787–2814. doi:10.1007/s00018-
617 013-1550-7
- 618 4. Lalonde J, Saia G, Gill G. Store-operated calcium entry promotes the degradation of
619 the transcription factor Sp4 in resting neurons. *Sci Signal. United States;* 2014;7:
620 ra51. doi:10.1126/scisignal.2005242
- 621 5. Hartmann J, Karl RM, Alexander RPD, Adelsberger H, Brill MS, Ruhlmann C, et al.
622 STIM1 controls neuronal Ca(2)(+) signaling, mGluR1-dependent synaptic
623 transmission, and cerebellar motor behavior. *Neuron. United States;* 2014;82: 635–
624 644. doi:10.1016/j.neuron.2014.03.027
- 625 6. Berna-Erro A, Braun A, Kraft R, Kleinschnitz C, Schuhmann MK, Stegner D, et al.
626 STIM2 Regulates Capacitive Ca²⁺ Entry in Neurons and Plays a Key Role in Hypoxic
627 Neuronal Cell Death. *Sci Signal.* 2009;2: ra67 LP-ra67. Available:
628 <http://stke.sciencemag.org/content/2/93/ra67.abstract>
- 629 7. Sun S, Zhang H, Liu J, Popugaeva E, Xu N-J, Feske S, et al. Reduced synaptic STIM2
630 expression and impaired store-operated calcium entry cause destabilization of
631 mature spines in mutant presenilin mice. *Neuron. United States;* 2014;82: 79–93.
632 doi:10.1016/j.neuron.2014.02.019
- 633 8. Park CY, Shcheglovitov A, Dolmetsch R. The CRAC channel activator STIM1 binds
634 and inhibits L-type voltage-gated calcium channels. *Science. United States;*
635 2010;330: 101–105. doi:10.1126/science.1191027
- 636 9. Wang Y, Deng X, Mancarella S, Hendron E, Eguchi S, Soboloff J, et al. The calcium
637 store sensor, STIM1, reciprocally controls Orai and CaV1.2 channels. *Science. United*
638 *States;* 2010;330: 105–109. doi:10.1126/science.1191086
- 639 10. Nguyen N, Biet M, Simard É, Béliveau É, Francoeur N, Guillemette G, et al. STIM1
640 participates in the contractile rhythmicity of HL-1 cells by moderating T-type Ca²⁺
641 channel activity. *Biochim Biophys Acta - Mol Cell Res.* 2013;1833: 1294–1303.
642 doi:<https://doi.org/10.1016/j.bbamcr.2013.02.027>
- 643 11. Jékely G. Global view of the evolution and diversity of metazoan neuropeptide
644 signaling. *Proc Natl Acad Sci.* 2013;110: 8702 LP-8707. Available:
645 <http://www.pnas.org/content/110/21/8702.abstract>
- 646 12. Elphick MR, Mirabeau O, Larhammar D. Evolution of neuropeptide signalling
647 systems. *J Exp Biol.* 2018;221: jeb151092. doi:10.1242/jeb.151092
- 648 13. Nassel DR, Winther AM. *Drosophila* neuropeptides in regulation of physiology and
649 behavior. *Prog Neurobiol.* 2010;92: 42–104. Available:
650 [http://www.ncbi.nlm.nih.gov/entrez/query.fcgi?cmd=Retrieve&db=PubMed&dopt=C](http://www.ncbi.nlm.nih.gov/entrez/query.fcgi?cmd=Retrieve&db=PubMed&dopt=Citation&list_uids=20447440)
651 [itation&list_uids=20447440](http://www.ncbi.nlm.nih.gov/entrez/query.fcgi?cmd=Retrieve&db=PubMed&dopt=Citation&list_uids=20447440)

- 652 14. Taghert PH, Nitabach MN. Peptide neuromodulation in invertebrate model systems.
653 Neuron. United States; 2012;76: 82–97. doi:10.1016/j.neuron.2012.08.035
- 654 15. Venkiteswaran G, Hasan G. Intracellular Ca²⁺ signaling and store-operated Ca²⁺
655 entry are required in Drosophila neurons for flight. Proc Natl Acad Sci U S A.
656 2009;106: 10326–10331. Available:
657 [http://www.ncbi.nlm.nih.gov/entrez/query.fcgi?cmd=Retrieve&db=PubMed&dopt=C](http://www.ncbi.nlm.nih.gov/entrez/query.fcgi?cmd=Retrieve&db=PubMed&dopt=Citation&list_uids=19515818)
658 [itation&list_uids=19515818](http://www.ncbi.nlm.nih.gov/entrez/query.fcgi?cmd=Retrieve&db=PubMed&dopt=Citation&list_uids=19515818)
- 659 16. Chakraborty S, Deb BK, Chorna T, Konieczny V, Taylor CW, Hasan G. Mutant IP₃
660 receptors attenuate store-operated Ca²⁺ entry by destabilizing STIM-Orai
661 interactions in Drosophila neurons. J Cell Sci. 2016; doi:10.1242/jcs.191585
- 662 17. Richhariya S, Jayakumar S, Kumar Sukumar S, Hasan G. dSTIM and Ral/Exocyst
663 Mediated Synaptic Release from Pupal Dopaminergic Neurons Sustains Drosophila
664 Flight. eNeuro. 2018;5. Available:
665 <http://eNeuro.org/content/early/2018/05/22/ENEURO.0455-17.2018.abstract>
- 666 18. Jayakumar S, Richhariya S, Deb BK, Hasan G. A Multicomponent Neuronal Response
667 Encodes the Larval Decision to Pupariate upon Amino Acid Starvation. J Neurosci.
668 2018;38: 10202 LP-10219. doi:10.1523/JNEUROSCI.1163-18.2018
- 669 19. Agrawal N, Venkiteswaran G, Sadaf S, Padmanabhan N, Banerjee S, Hasan G.
670 Inositol 1,4,5-trisphosphate receptor and dSTIM function in Drosophila insulin-
671 producing neurons regulates systemic intracellular calcium homeostasis and flight. J
672 Neurosci. 2010;30: 1301–1313. Available:
673 [http://www.ncbi.nlm.nih.gov/entrez/query.fcgi?cmd=Retrieve&db=PubMed&dopt=C](http://www.ncbi.nlm.nih.gov/entrez/query.fcgi?cmd=Retrieve&db=PubMed&dopt=Citation&list_uids=20107057)
674 [itation&list_uids=20107057](http://www.ncbi.nlm.nih.gov/entrez/query.fcgi?cmd=Retrieve&db=PubMed&dopt=Citation&list_uids=20107057)
- 675 20. Chakraborty S, Hasan G. IP₃R, store-operated Ca²⁺ entry and neuronal Ca²⁺
676 homeostasis in Drosophila. Biochem Soc Trans. 2012/01/21. 2012;40: 279–281.
677 doi:10.1042/BST20110618BST20110618 [pii]
- 678 21. Gopurappilly R, Deb BK, Chakraborty P, Hasan G. Stable STIM₁ Knockdown in Self-
679 Renewing Human Neural Precursors Promotes Premature Neural Differentiation
680 [Internet]. Frontiers in Molecular Neuroscience . 2018. p. 178. Available:
681 <https://www.frontiersin.org/article/10.3389/fnmol.2018.00178>
- 682 22. Megha, Hasan G. IP₃R-mediated Ca²⁺ release regulates protein metabolism in
683 Drosophila neuroendocrine cells: implications for development under nutrient stress.
684 Development. England; 2017;144: 1484–1489. doi:10.1242/dev.145235
- 685 23. Agrawal T, Sadaf S, Hasan G. A genetic RNAi screen for IP₃/Ca²⁺(+) coupled GPCRs
686 in Drosophila identifies the PdfR as a regulator of insect flight. PLoS Genet.
687 2013/10/08. 2013;9: e1003849. doi:10.1371/journal.pgen.1003849PGENETICS-D-13-
688 01291 [pii]
- 689 24. Nassel DR, Enell LE, Santos JG, Wegener C, Johard HA. A large population of diverse
690 neurons in the Drosophila central nervous system expresses short neuropeptide F,
691 suggesting multiple distributed peptide functions. BMC Neurosci. 2008;9: 90.
692 Available:
693 [http://www.ncbi.nlm.nih.gov/entrez/query.fcgi?cmd=Retrieve&db=PubMed&dopt=C](http://www.ncbi.nlm.nih.gov/entrez/query.fcgi?cmd=Retrieve&db=PubMed&dopt=Citation&list_uids=18803813)
694 [itation&list_uids=18803813](http://www.ncbi.nlm.nih.gov/entrez/query.fcgi?cmd=Retrieve&db=PubMed&dopt=Citation&list_uids=18803813)
- 695 25. Rhea JM, Wegener C, Bender M. The proprotein convertase encoded by *amontillado*
696 (*amon*) is required in Drosophila corpora cardiaca endocrine cells producing the
697 glucose regulatory hormone AKH. PLoS Genet. 2010;6: e1000967. Available:
698 <http://www.ncbi.nlm.nih.gov/entrez/query.fcgi?cmd=Retrieve&db=PubMed&dopt=C>

- 699 itation&list_uids=20523747
700 26. Pathak T, Agrawal T, Richhariya S, Sadaf S, Hasan G. Store-Operated Calcium Entry
701 through Orai Is Required for Transcriptional Maturation of the Flight Circuit in
702 *Drosophila*. *J Neurosci*. United States; 2015;35: 13784–13799.
703 doi:10.1523/JNEUROSCI.1680-15.2015
704 27. Lee KS, You KH, Choo JK, Han YM, Yu K. *Drosophila* short neuropeptide F regulates
705 food intake and body size. *J Biol Chem*. 2004;279: 50781–50789. Available:
706 [http://www.ncbi.nlm.nih.gov/entrez/query.fcgi?cmd=Retrieve&db=PubMed&dopt=C](http://www.ncbi.nlm.nih.gov/entrez/query.fcgi?cmd=Retrieve&db=PubMed&dopt=Citation&list_uids=15385546)
707 itation&list_uids=15385546
708 28. Subramanian M, Jayakumar S, Richhariya S, Hasan G. Loss of IP₃ receptor function in
709 neuropeptide secreting neurons leads to obesity in adult *Drosophila*. *BMC Neurosci*.
710 2013/12/20. 2013;14: 157. doi:10.1186/1471-2202-14-157 [pii]
711 29. Agrawal N, Padmanabhan N, Hasan G. Inositol 1,4,5- trisphosphate receptor function
712 in *Drosophila* insulin producing cells. *PLoS One*. 2009;4: e6652. Available:
713 [http://www.ncbi.nlm.nih.gov/entrez/query.fcgi?cmd=Retrieve&db=PubMed&dopt=C](http://www.ncbi.nlm.nih.gov/entrez/query.fcgi?cmd=Retrieve&db=PubMed&dopt=Citation&list_uids=19680544)
714 itation&list_uids=19680544
715 30. Choi YJ, Lee G, Hall JC, Park JH. Comparative analysis of *Corazonin*-encoding genes
716 (*Crz*'s) in *Drosophila* species and functional insights into *Crz*-expressing neurons. *J*
717 *Comp Neurol*. United States; 2005;482: 372–385. doi:10.1002/cne.20419
718 31. Rao S, Lang C, Levitan ES, Deitcher DL. Visualization of neuropeptide expression,
719 transport, and exocytosis in *Drosophila melanogaster*. *J Neurobiol*. United States;
720 2001;49: 159–172.
721 32. Fosque BF, Sun Y, Dana H, Yang C-T, Ohyama T, Tadross MR, et al. Neural circuits.
722 Labeling of active neural circuits in vivo with designed calcium integrators. *Science*.
723 United States; 2015;347: 755–760. doi:10.1126/science.1260922
724 33. Veenstra JA. Peptidergic paracrine and endocrine cells in the midgut of the fruit fly
725 maggot. *Cell Tissue Res*. 2009;336: 309–323. Available:
726 [http://www.ncbi.nlm.nih.gov/entrez/query.fcgi?cmd=Retrieve&db=PubMed&dopt=C](http://www.ncbi.nlm.nih.gov/entrez/query.fcgi?cmd=Retrieve&db=PubMed&dopt=Citation&list_uids=19319573)
727 itation&list_uids=19319573
728 34. Wegener C, Herbert H, Kahnt J, Bender M, Rhea JM. Deficiency of prohormone
729 convertase *dPC2* (*AMONTILLADO*) results in impaired production of bioactive
730 neuropeptide hormones in *Drosophila*. *J Neurochem*. 2011;118: 581–595. Available:
731 [http://www.ncbi.nlm.nih.gov/entrez/query.fcgi?cmd=Retrieve&db=PubMed&dopt=C](http://www.ncbi.nlm.nih.gov/entrez/query.fcgi?cmd=Retrieve&db=PubMed&dopt=Citation&list_uids=21138435)
732 itation&list_uids=21138435
733 35. Luo J, Liu Y, Nassel DR, Nässel DR. Insulin/IGF-regulated size scaling of
734 neuroendocrine cells expressing the bHLH transcription factor *Dimmed* in
735 *Drosophila*. *PLoS Genet*. 2014/01/05. Public Library of Science; 2013;9: e1004052.
736 doi:10.1371/journal.pgen.1004052
737 36. Park D, Veenstra JA, Park JH, Taghert PH. Mapping peptidergic cells in *Drosophila*:
738 where *DIMM* fits in. *PLoS One*. 2008;3: e1896. Available:
739 [http://www.ncbi.nlm.nih.gov/entrez/query.fcgi?cmd=Retrieve&db=PubMed&dopt=C](http://www.ncbi.nlm.nih.gov/entrez/query.fcgi?cmd=Retrieve&db=PubMed&dopt=Citation&list_uids=18365028)
740 itation&list_uids=18365028
741 37. Richhariya S, Jayakumar S, Abruzzi K, Rosbash M, Hasan G. A pupal transcriptomic
742 screen identifies *Ral* as a target of store-operated calcium entry in *Drosophila*
743 neurons. *Sci Rep*. The Author(s); 2017;7: 42586. Available:
744 <http://dx.doi.org/10.1038/srep42586>
745 38. Wong MY, Cavolo SL, Levitan ES. Synaptic neuropeptide release by dynamin-

- 746 dependent partial release from circulating vesicles. *Mol Biol Cell*. United States;
747 2015;26: 2466–2474. doi:10.1091/mbc.E15-01-0002
- 748 39. McNabb SL, Truman JW. Light and peptidergic eclosion hormone neurons stimulate
749 a rapid eclosion response that masks circadian emergence in *Drosophila*. *J Exp Biol*.
750 2008;211: 2263–2274. doi:10.1242/jeb.015818
- 751 40. Klose M, Duvall L, Li W, Liang X, Ren C, Steinbach JH, et al. Functional PDF Signaling
752 in the *Drosophila* Circadian Neural Circuit Is Gated by Ral A-Dependent Modulation.
753 *Neuron*. 2016/05/05. 2016;90: 781–794. doi:10.1016/j.neuron.2016.04.002
- 754 41. Nässel DR. Neuropeptide signaling near and far: how localized and timed is the
755 action of neuropeptides in brain circuits? *Invertebr Neurosci*. 2009;9: 57.
756 doi:10.1007/s10158-009-0090-1
- 757 42. Kubrak OI, Lushchak O V, Zandawala M, Nässel DR. Systemic corazonin signalling
758 modulates stress responses and metabolism in *Drosophila*. *Open Biol*. The Royal
759 Society; 2016;6: 160152. doi:10.1098/rsob.160152
- 760 43. Chintapalli VR, Wang J, Dow JAT. Using FlyAtlas to identify better *Drosophila*
761 *melanogaster* models of human disease. *Nat Genet*. United States; 2007;39: 715–720.
762 doi:10.1038/ng2049
- 763 44. Pulver SR, Pashkovski SL, Hornstein NJ, Garrity PA, Griffith LC. Temporal dynamics
764 of neuronal activation by Channelrhodopsin-2 and TRPA1 determine behavioral
765 output in *Drosophila* larvae. *J Neurophysiol*. 2009/04/01. American Physiological
766 Society; 2009;101: 3075–3088. doi:10.1152/jn.00071.2009
- 767 45. Dawydow A, Gueta R, Ljaschenko D, Ullrich S, Hermann M, Ehmann N, et al.
768 Channelrhodopsin-2–XXL, a powerful optogenetic tool for low-light applications.
769 *Proc Natl Acad Sci*. 2014;111: 13972 LP-13977. Available:
770 <http://www.pnas.org/content/111/38/13972.abstract>
- 771 46. Lee G, Kim KM, Kikuno K, Wang Z, Choi YJ, Park JH. Developmental regulation and
772 functions of the expression of the neuropeptide corazonin in *Drosophila*
773 *melanogaster*. *Cell Tissue Res*. 2008;331: 659–673. Available:
774 [http://www.ncbi.nlm.nih.gov/entrez/query.fcgi?cmd=Retrieve&db=PubMed&dopt=C](http://www.ncbi.nlm.nih.gov/entrez/query.fcgi?cmd=Retrieve&db=PubMed&dopt=Citation&list_uids=18087727)
775 [itation&list_uids=18087727](http://www.ncbi.nlm.nih.gov/entrez/query.fcgi?cmd=Retrieve&db=PubMed&dopt=Citation&list_uids=18087727)
- 776 47. Kapan N, Lushchak O V, Luo J, Nässel DR. Identified peptidergic neurons in the
777 *Drosophila* brain regulate insulin-producing cells, stress responses and metabolism
778 by coexpressed short neuropeptide F and corazonin. *Cell Mol Life Sci*. 2012;69: 4051–
779 4066. doi:10.1007/s00018-012-1097-z
- 780 48. Johnson EC, Kazgan N, Bretz CA, Forsberg LJ, Hector CE, Worthen RJ, et al. Altered
781 Metabolism and Persistent Starvation Behaviors Caused by Reduced AMPK Function
782 in *Drosophila*. Hassan BA, editor. *PLoS One*. San Francisco, USA: Public Library of
783 Science; 2010;5: e12799. doi:10.1371/journal.pone.0012799
- 784 49. Tayler TD, Pacheco DA, Hergarden AC, Murthy M, Anderson DJ. A neuropeptide
785 circuit that coordinates sperm transfer and copulation duration in *Drosophila*. *Proc*
786 *Natl Acad Sci U S A*. National Academy of Sciences; 2012;109: 20697–20702.
787 doi:10.1073/pnas.1218246109
- 788 50. McClure KD, Heberlein U. A Small Group of Neurosecretory Cells Expressing the
789 Transcriptional Regulator apontic and the Neuropeptide corazonin Mediate Ethanol
790 Sedation in *Drosophila*. *J Neurosci*. Society for Neuroscience; 2013;33: 4044–4054.
791 doi:10.1523/JNEUROSCI.3413-12.2013
- 792 51. Sha K, Choi S-H, Im J, Lee GG, Loeffler F, Park JH. Regulation of Ethanol-Related

- 793 Behavior and Ethanol Metabolism by the Corazonin Neurons and Corazonin
794 Receptor in *Drosophila melanogaster*. PLoS One. Public Library of Science; 2014;9:
795 e87062. Available: <https://doi.org/10.1371/journal.pone.0087062>
796 52. Lee KS, Kwon OY, Lee JH, Kwon K, Min KJ, Jung SA, et al. *Drosophila* short
797 neuropeptide F signalling regulates growth by ERK-mediated insulin signalling. Nat
798 Cell Biol. 2008;10: 468–475. Available:
799 [http://www.ncbi.nlm.nih.gov/entrez/query.fcgi?cmd=Retrieve&db=PubMed&dopt=C](http://www.ncbi.nlm.nih.gov/entrez/query.fcgi?cmd=Retrieve&db=PubMed&dopt=Citation&list_uids=18344986)
800 [itation&list_uids=18344986](http://www.ncbi.nlm.nih.gov/entrez/query.fcgi?cmd=Retrieve&db=PubMed&dopt=Citation&list_uids=18344986)
801 53. Selcho M, Millán C, Palacios-Muñoz A, Ruf F, Ubillo L, Chen J, et al. Central and
802 peripheral clocks are coupled by a neuropeptide pathway in *Drosophila*. Nat
803 Commun. The Author(s); 2017;8: 15563. Available:
804 <http://dx.doi.org/10.1038/ncomms15563>
805 54. Chen W, Shi W, Li L, Zheng Z, Li T, Bai W, et al. Regulation of sleep by the short
806 neuropeptide F (sNPF) in *Drosophila melanogaster*. Insect Biochem Mol Biol.
807 England; 2013;43: 809–819. doi:10.1016/j.ibmb.2013.06.003
808 55. Shang Y, Donelson NC, Vecsey CG, Guo F, Rosbash M, Griffith LC. Short
809 neuropeptide F is a sleep-promoting inhibitory modulator. Neuron. United States;
810 2013;80: 171–183. doi:10.1016/j.neuron.2013.07.029
811 56. Veenstra JA. Does corazonin signal nutritional stress in insects? Insect Biochem Mol
812 Biol. 2009;39: 755–762. Available:
813 [http://www.ncbi.nlm.nih.gov/entrez/query.fcgi?cmd=Retrieve&db=PubMed&dopt=C](http://www.ncbi.nlm.nih.gov/entrez/query.fcgi?cmd=Retrieve&db=PubMed&dopt=Citation&list_uids=19815069)
814 [itation&list_uids=19815069](http://www.ncbi.nlm.nih.gov/entrez/query.fcgi?cmd=Retrieve&db=PubMed&dopt=Citation&list_uids=19815069)
815 57. Mishra D, Miyamoto T, Rezenom YH, Broussard A, Yavuz A, Slone J, et al. The
816 Molecular Basis of Sugar Sensing in *Drosophila* Larvae. Curr Biol.
817 Elsevier; 2013;23: 1466–1471. doi:10.1016/j.cub.2013.06.028
818 58. Miyamoto T, Amrein H. Diverse roles for the *Drosophila* fructose sensor Gr43a. Fly
819 (Austin). Landes Bioscience; 2014;8: 19–25. doi:10.4161/fly.27241
820 59. Johnson EC, Shafer OT, Trigg JS, Park J, Schooley DA, Dow JA, et al. A novel diuretic
821 hormone receptor in *Drosophila*: evidence for conservation of CGRP signaling. J Exp
822 Biol. England; 2005;208: 1239–1246. doi:10.1242/jeb.01529
823 60. Hartenstein V. The neuroendocrine system of invertebrates: a developmental and
824 evolutionary perspective. J Endocrinol. England; 2006;190: 555–570.
825 doi:10.1677/joe.1.06964
826 61. Onaka T, Takayanagi Y, Leng G. Metabolic and stress-related roles of prolactin-
827 releasing peptide. Trends Endocrinol Metab. 2010;21: 287–293.
828 doi:<https://doi.org/10.1016/j.tem.2010.01.005>
829 62. van den Pol AN. Neuropeptide transmission in brain circuits. Neuron. United States;
830 2012;76: 98–115. doi:10.1016/j.neuron.2012.09.014
831 63. Shakiryanova D, Zettel GM, Gu T, Hewes RS, Levitan ES. Synaptic neuropeptide
832 release induced by octopamine without Ca²⁺ entry into the nerve terminal. Proc Natl
833 Acad Sci U S A. 2011;108: 4477–4481. Available:
834 [http://www.ncbi.nlm.nih.gov/entrez/query.fcgi?cmd=Retrieve&db=PubMed&dopt=C](http://www.ncbi.nlm.nih.gov/entrez/query.fcgi?cmd=Retrieve&db=PubMed&dopt=Citation&list_uids=21368121)
835 [itation&list_uids=21368121](http://www.ncbi.nlm.nih.gov/entrez/query.fcgi?cmd=Retrieve&db=PubMed&dopt=Citation&list_uids=21368121)
836 64. Wang Y, Wu Q, Hu M, Liu B, Chai Z, Huang R, et al. Ligand- and voltage-gated Ca²⁺
837 channels differentially regulate the mode of vesicular neuropeptide release in
838 mammalian sensory neurons. Sci Signal. 2017;10: eaal1683. Available:
839 <http://stke.sciencemag.org/content/10/484/eaal1683.abstract>

- 840 65. Zhou Q, Yen A, Rymarczyk G, Asai H, Trengrove C, Aziz N, et al. Impairment of
841 PARK14-dependent Ca(2+) signalling is a novel determinant of Parkinson's disease.
842 Nat Commun. England; 2016;7: 10332. doi:10.1038/ncomms10332
843 66. Secondo A, Bagetta G, Amantea D. On the Role of Store-Operated Calcium Entry in
844 Acute and Chronic Neurodegenerative Diseases. Front Mol Neurosci. Switzerland;
845 2018;11: 87. doi:10.3389/fnmol.2018.00087
846 67. Popugaeva E, Bezprozvanny I. Role of endoplasmic reticulum Ca²⁺ signaling in the
847 pathogenesis of Alzheimer disease. Front Mol Neurosci. Switzerland; 2013;6: 29.
848 doi:10.3389/fnmol.2013.00029
849 68. Wegener C, Neupert S, Predel R. Direct MALDI-TOF mass spectrometric peptide
850 profiling of neuroendocrine tissue of Drosophila. Methods Mol Biol. 2010;615: 117–
851 127. Available:
852 [http://www.ncbi.nlm.nih.gov/entrez/query.fcgi?cmd=Retrieve&db=PubMed&dopt=C](http://www.ncbi.nlm.nih.gov/entrez/query.fcgi?cmd=Retrieve&db=PubMed&dopt= Citation&list_uids=20013204)
853 [itation&list_uids=20013204](http://www.ncbi.nlm.nih.gov/entrez/query.fcgi?cmd=Retrieve&db=PubMed&dopt=Citation&list_uids=20013204)
854
855